CXXC5 Plays a Role as a Transcription Activator for Myelin Genes on Oligodendrocyte Differentiation

Mi-Yeon Kim,[1,2] Hyun-Yi Kim,[1,2] Jiso Hong,[3] Daesoo Kim,[3] Hyojung Lee,[1,2] Eunji Cheong,[1,2] Yangsin Lee,[4] Jürgen Roth,[4] Dong Goo Kim,[5] Do Sik Min,[1,6] and Kang-Yell Choi[1,2]

Myelination in corpus callosum plays important role for normal brain functions by transferring neurological information between various brain regions. However, the factors controlling expression of myelin genes in myelination are poorly understood. Here, CXXC5, a recently identified protein with CXXC-type zinc finger DNA binding motif, was characterized as a transcriptional activator of major myelin genes. We identified expression of CXXC5 expression was increased by Wnt/β-catenin signaling. CXXC5 specifically expressed in the white matter induced expression of myelin genes through the direct binding of CXXC DNA-binding motif of CXXC5 on the *MBP* promoter. During the differentiation of neural stem cells (NSCs) of *CXXC5*$^{-/-}$ mice, the expressions of myelin genes were simultaneously reduced. The *CXXC5*$^{-/-}$ mice exhibited severely reduction of myelin genes expression in corpus callosum as well as abnormalities in myelin structure. The disrupted structural integrity of myelin in the *CXXC5*$^{-/-}$ mice resulted in reduced electrical conduction amplitudes at corpus callosum. These findings indicate that the regulation of myelin genes expression by CXXC5 is important for forming myelin structure involved with axonal electrical signal transfer in the corpus callosum.

GLIA 2016;64:350–362

Key words: CXXC5, oligodendrocyte, transcription factor, neural stem cell, Wnt/β-catenin signaling

Introduction

Oligodendrocytes synthesize the myelin sheath which insulating neural axons and supporting rapid neural action potential propagation in the central nervous system (CNS) (Deber and Reynolds, 1991; Inouye and Kirschner, 1991). Myelinated axons consists white matter involved in the transmission of electrical signals between different areas of the brain. The myelination abnormalities that interrupt nerve impulse transfer can cause neurological disorders, such as depression, bipolar disorder (Brambilla et al., 2009; Mahon et al., 2010), autism (Vourc'h et al., 2003), schizophrenia (Haroutunian et al., 2014; Vourc'h et al., 2003), and neuropathy (Richardson et al., 2006). Thus, the identification and characterization of the genes involved in the myelination are important for understanding the complex processes of brain development.

Oligodendrocytes are generated from oligodendrocyte progenitor cells (OPCs) which are differentiated from neural stem cells (NSCs) in the ventricular zone (VZ) of brain (Lee et al., 2000). The myelination of oligodendrocytes is mediated by the activation of various myelin genes, such as *myelin basic protein* (*MBP*), *proteolipid protein* (*PLP*), *myelin associate protein (MAG)*, and *myelin oligodendrocyte glycoprotein* (*MOG*), which are involved in myelin structural integrity (Aggarwal et al., 2011; Rosenbluth et al., 2006; Seiwa et al., 2000). The Wnt/β-catenin signaling is involved in myelin

View this article online at wileyonlinelibrary.com. DOI: 10.1002/glia.22932

Published online October 14, 2015 in Wiley Online Library (wileyonlinelibrary.com). Received June 3, 2015, Accepted for publication Sep 24, 2015.

Address correspondence to Kang-Yell Choi; College of Life Science and Biotechnology, Yonsei University, Seoul, 120-749, Korea. E-mail:kychoi@yonsei.ac.kr

From the [1]Translational Research Center for Protein Function Control, Yonsei University, Seoul, 120-749, Korea; [2]Department of Biotechnology, College of Life Science and Biotechnology, Yonsei University, Seoul, 120-749, Korea; [3]Biological Sciences, Korea Advanced Institute of Science and Technology (KAIST), Daejeon, 305-701, Korea; [4]Department of Integrated OMICS For Biomedical Science, WCU Program of Graduate School, Yonsei University, Seoul, 120-749, Korea; [5]Department of Pharmacology, Brain Research Institute, Brain Korea 21 Project for Medical Science, Severance Biomedical Science Institute, Yonsei University, College of Medicine, Seoul, 120-749, Korea; [6]Department of Molecular Biology, College of Natural Science, Pusan National University, Busan, 609-735, Korea

Additional Supporting Information may be found in the online version of this article.

gene expression (Guo et al., 2015; Langseth et al., 2010; Tawk et al., 2011). In peripheral nervous system (PNS), the Wnt/β-catenin signaling directly induces expressions of myelin genes such as peripheral myelin protein-22 (PMP22) or myelin protein zero (MPZ) through binding of β-catenin/TCF complex on promoters of PMP22 or MPZ (Makoukji et al., 2011; Tawk et al., 2011). However transcriptional control of myelin genes in oligodendrocyte remain poorly understood.

CXXC5 is a recently identified protein with CXXC-type zinc finger DNA-binding motifs and nuclear localization sequences (NLS) (Cokol et al., 2000; Pendino et al., 2009). CXXC5 was identified as a nuclear factor activating several genes, such as *P53, COX4I2*, and *Flk1* (Aras et al., 2013; Kim et al. 2014; Zhang et al., 2009), and its role in the cytosol as a negative regulator for Wnt/β-catenin signaling was also identified (Kim et al. 2015; Kim et al. 2010a). CXXC5 was identified a potential target of BMP4 signaling in neural stem cells functioning in brain (Andersson et al., 2009). CXXC5 was also identified as a potential target gene of β-catenin (Bottomly et al., 2010). In addition, *CXXC5* was also identified as a weakly expressed gene in global gene expression profile of bipolar disorder patient compared with their co-twins (Matigian et al., 2007). However, the role of CXXC5 as a transcription factor in nervous system is not known.

In the present study, using a mouse model, we identified and characterized the CXXC5 as a transcription factor that activated a series of genes involved in myelination and its role in interhemispheric function. The expression of CXXC5 was increased by Wnt/β-catenin signaling in NSCs together with the myelin genes. In addition, CXXC5 expression increased during the differentiation of NSCs and during the brain development of mice, correlating with the expression of multiple myelin genes. In addition, *in vitro* DNA binding analyses were used to characterize CXXC5 as a direct transcriptional activator for *MBP*. The *in vivo* role of CXXC5 as an activator for myelin genes was also demonstrated by the severe reductions in the expression of *MBP* and other myelin genes in the corpus callosum of *CXXC5*$^{-/-}$ mice. The abolishment of myelin structural integrity by loss of *CXXC5* was demonstrated by electron microscopy analyses, and subsequent outcome was shown by a reduction in conduction amplitudes through axon bundles. Together, these results show that CXXC5 maintained myelin structural integrity for transferring the electrical signal on corpus callosum in developmental stages of mice.

Materials and Methods

Animals

The *CXXC5*$^{-/-}$ mice were established in previous study (Kim et al. 2014; Kim et al. 2015). All of the mice used in this study were treated according to protocols approved by the Institutional Animal Care and Use Committee (IACUC) of Yonsei University, Seoul, Korea. All mice had unlimited access to water and breeding chow and male mice were used for every experiment.

Cell Culture

The primary NSCs were isolated from embryonic day 14.5 (E14.5) *CXXC5*$^{-/-}$ and *CXXC5*$^{+/+}$ mice, and neurospheres were cultured as previously described (Kim et al. 2010b; Kim et al. 2013). For neurosphere culture, the cells were mechanically dissociated from brain tissue and grown in N2 medium in 25 cm^2 flasks (Nunc, Pittsburgh, PA) in suspension. About 10 ng/mL human bFGF (Peprotech, Princeton, NJ) and 20 ng/mL human EGF (Peprotech) were added to the media to allow the cells to form neurospheres. For analyses, NSCs were cultured as monolayer. For differentiation of NSCs, the neurospheres were dissociated with TrypLE (Gibco, Carlsbad, CA), plated on 15 μg/mL poly-L-ornithine- (Sigma-Aldrich, St. Louis, MO) and 10 μg/mL fibronectin (Gibco)-coated plates, and cultured in bFGF- and EGF-depleted N2 medium for 4 days.

The OPCs (Oli-neu cell line) were provided by Dr. Jacqueline Trotter at The University of Mainz, Germany. OPCs were grown in Oli-neu medium containing Sato's ingredients and 2% horse serum in DMEM/F12 (1:1) (Invitrogen, Carlsbad, CA) on 1 mg/mL poly-L-lysine-coated dishes (Jung et al., 1995). For oligodendrocyte differentiation, 1 mM cAMP (Sigma-Aldrich) was added for 6 days. For transient transfection, the cells were cultured for 1 day and then transfected with the required plasmids using the Lipofectamine Plus transfection reagent (Invitrogen) according to the manufacturer's instructions.

Plasmids and Small Interfering RNA (siRNA)

The pGL3-MBP promoter was obtained from Dr. Li-Jin Chew (Chew et al., 2010), and serially deleted MBP promoter constructs in the pGL3 vector were provided by Dr. Robin Miskimins (Wei et al., 2003). The pGL3-PLP1 promoter was obtained from Dr. Charbel Massaad (Tawk et al., 2011). The pcDNA 3.1-flag-CXXC5 and pcDNA 3.1-myc-CXXC5, CXXC5 overexpression vectors, as well as the mutant constructs [pcDNA 3.1-myc-CXXC5 (C263/266R), pcDNA3.1-myc-CXXC5 (C275/278R), and pcDNA 3.1-myc-CXXC5 (C263/266R, C275/278R)] were described in a previous study (Kim et al., 2010a). The sequences of *β-catenin* siRNA were as follows: sense: 5′-AUU ACA UCC GGU UGU GAC GUC CC-3′, anti-sense: 5′-GGG ACG UUC ACA CCG GAU UGU AU-3′.

Reporter Analysis

NSCs and OPCs were cultured for 1 day and then transfected with pGL3-MBP, pGL3-PLP1, or serially deleted MBP promoter constructs in pGL3, together with β-gal-pCMV, using the Lipofectamine Plus transfection reagent. The transfected cells were further cultured for 1–4 days before harvesting for the reporter assay. The harvested cells were resuspended in lysis buffer (Promega, Madison, WI), and the luciferase activities were measured and normalized using β-galactosidase activities as an internal control (Yang et al., 2009).

Immunohistochemical Analysis

The immunohistochemical analysis was performed as previously described (Jeong et al., 2012). *CXXC5*$^{+/+}$ mice and *CXXC5*$^{-/-}$ mice brain tissues were fixed in 4% paraformaldehyde and processed for paraffin sections using a RM2245 microtome (Leica Microsystems, Wetzlar, Germany). The tissue sections were deparaffinized, and antigen retrieval was performed in citrate buffer (pH 6.0). For immune staining, the sections were incubated with anti-CXXC5 (Kim et al. 2015), anti-MBP, anti-c-Fos or anti-GFAP antibodies. This step was followed by incubation with Alexa Fluor 488-conjugated anti-goat IgG or Alexa Fluor 488-conjugated anti-rat IgG secondary antibodies. The sections were counterstained with DAPI. The immunofluorescent images were captured using a LSM 510 META confocal microscope. For diaminobenzidine (DAB) staining, immunohistochemistry was performed with the peroxidase substrate in the DAB kit (Vector Laboratories Inc., Burlingame, CA). The samples were observed with an ECLIPSE TE2000-U microscope (Nikon, Tokyo, Japan).

Chromatin Immunoprecipitation (ChIP) Assay

NSCs and OPCs were transfected with pcDNA3.1-myc-CXXC5, pcDNA3.1-myc-CXXC5, pcDNA 3.1-myc-CXXC5 (C263/266R), pcDNA3.1-myc-CXXC5 (C275/278R), or pcDNA 3.1-myc-CXXC5 (C263/266R, C275/278R), and then grown under non-differentiation conditions for 1 day. One percent formaldehyde was used to treat cells for 30 min at 37°C. The cells were then washed twice in ice-cold PBS containing 1 mM phenylmethanesulfonyl fluoride (PMSF) and then collected by scraping in lysis buffer (1% SDS, 10 mM EDTA, 50 mM Tris, pH 8.0) on ice. The lysates were sonicated 5× for 30 seconds at 50% amplitude and 0.5 cycles, while keeping the samples on ice. The samples were then diluted with ChIP dilution buffer [1% SDS, 1% Triton X-100, 1.2 mM EDTA, 16.7 mM Tris (pH 8.0), and 167 mM NaCl] containing 1 mM PMSF followed by incubation overnight at 4°C. The samples were then incubated with 3 μg of anti-myc antibody (Santa Cruz Biotechnology) or anti-mouse IgG (Santa Cruz Biotechnology) followed by incubation with 20 μL of salmon sperm DNA/protein A agarose beads (Millipore, Billerica, MA) overnight at 4°C. The DNA–protein complex was eluted with elution buffer (1% SDS and 0.1 M $NaHCO_3$) and pooled. The complexes were then reverse crosslinked at 65°C for 4 h, and the DNA was purified using phenol-chloroform and subjected to PCR amplification. The primer sets are shown in Supporting Information Table 5. The quantitative ChIP assay was performed as previously described (Jeon et al., 2008).

Transmission Electron Microscopy

The mice were euthanized using CO_2 gas. The brains were quickly removed, and thin slices (~1 mm thickness) containing the corpus callosum were cut. The slices were then fixed in 2% formaldehyde (freshly prepared from paraformaldehyde) and 0.5% glutaraldehyde in 0.1 M cacodylate buffer (pH 7.4), initially at 37°C for 4 h, and then rinsed in buffer. Pieces of the corpus callosum (~1 mm^3) were post-fixed in 1% osmium tetroxide in 0.1 M cacodylate buffer (pH 7.4) for 1 h. Following rinses with buffer, the tissue pieces were dehydrated in a graded series of ethanol and embedded in Epon-Araldite according to standard protocols.

Ultrathin sections (80 nm) were cut with a diamond knife (Diatome, Biel, Switzerland) using a Leica EM UC6 ultramicrotome (Leica Microsystems, Wetzlar, Germany) and stained with lead citrate and uranyl acetate. Ultrathin sections were observed with a Hitachi H-7650 electron microscope at 80 kV. The images were recorded using an 11-megapixel CCD XR611-M digital camera (Advanced Microscopy Techniques, Woburn, MA). The figures were generated using Photoshop (Adobe Systems, Inc. Mountain View, CA). The myelin thickness was estimated by the g-ratio (Paus and Toro, 2009), which is the ratio of individual axon diameters to myelinated fiber diameters.

Statistical Methods

All experiments were performed independently three times at least. The results are expressed as the mean ± standard error of the mean (SEM) of three different experiments for each condition. The each data was statistically analyzed using Student's *t*-test or one-way ANOVA test. $^{*}P < 0.05$, $^{**}P < 0.01$, $^{***}P < 0.005$.

Results

CXXC5 Expression Was Increased by Wnt/β-Catenin, and Myelin Genes Were Increased Together with the CXXC5 in Differentiation Induced NSCs

Both protein and transcription (mRNA and promoter activity) levels of CXXC5 increased by activated Wnt/β-catenin signaling (Fig. 1A,B). The Wnt3a-dependent increments of the expression CXXC5 was abolished by siRNA mediated β-catenin knock down (Fig. 1C,D). During the differentiation of NSCs, both mRNA and protein levels of CXXC5 were increased in differentiation condition by time-dependently (Fig. 1E,F). In addition, CXXC5 was accumulated in the nuclei of NSCs, whose differentiation was induced by the depletion of growth factors and differentiated into oligodendrocyte monitored by MBP expression (Fig. 1G).

The role of CXXC5 in oligodendrocyte differentiation, not the other lineages, was confirmed by immunocytochemical analysis in NSCs, derived from *CXXC5*$^{+/+}$ or *CXXC5*$^{-/-}$ mice, grown under differentiation conditions (Fig. 1H). The expression of MBP, oligodendrocyte marker, was reduced in *CXXC5*$^{-/-}$ NSCs compared with *CXXC5*$^{+/+}$ NSCs. However, the expression of neural marker, Tuj1, and astrocyte marker, GFAP, were not changed (Fig. 1I).

CXXC5 is Involved in the Oligodendrocyte Differentiation of NSCs

To identify genes regulated by CXXC5 during the differentiation of NSCs, we performed microarray analyses using differentiation-induced NSCs isolated from the *CXXC5*$^{+/+}$ and *CXXC5*$^{-/-}$ mice, with the differentiation performed via the depletion of growth factors. We found that 38 genes were

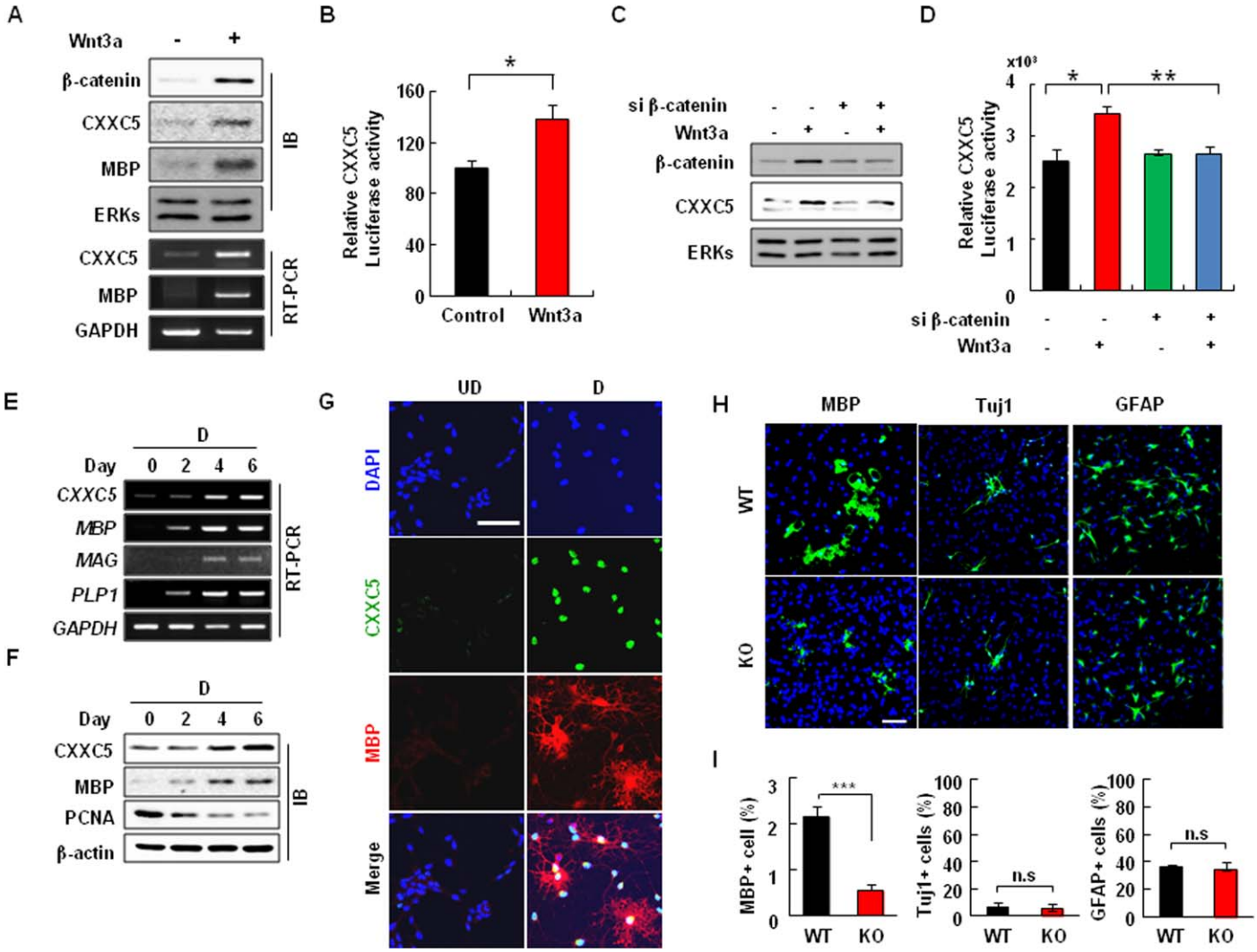

FIGURE 1: CXXC5 is induced by Wnt/β-catenin signaling, and its level is increased during the oligodendrocyte differentiation. A, B: NSCs were cultured on poly-L-ornithine- and fibronectin-coated cover slides and grown in non-differentiation condition with 50 ng/ml of Wnt3a for 4 days. A: The indicated proteins and mRNAs were detected using immunoblotting (IB) and RT-PCR, respectively. B: NSCs were transfected with pGL3-CXXC5 and the promoter activities were analyzed as described in "Materials and Methods." C, D: NSCs were transfected with 100 nM of *β-catenin* siRNA. After 24 h, 50 ng/mL of Wnt3a were treated for 4 days. C: The indicated proteins were detected using immunoblotting. D: NSCs were transfected with pGL3-CXXC5 and the promoter activities were analyzed. P values were obtained by Student's *t*-test (control vs. Wnt3a treated group, Wnt3a treated group vs. Vwt3a and siβ-catenin treated group). E, F: The mRNAs and proteins were isolated from differentiated NSCs isolated from E14.5 mice. The indicated mRNAs and proteins were detected using RT-PCR (E) and immunoblotting (IB) (F), respectively. G: NSCs were cultured on poly-L-ornithine- and fibronectin-coated cover slides and grown in N2 medium with or without bFGF and EGF for 4 days. The cells were subjected to immunofluorescent staining to detect MBP (*red*), and CXXC5 (*green*). Scale bar, 20 μm. H: NSCs from *CXXC5*$^{+/+}$ or *CXXC5*$^{-/-}$ were cultured in differentiation condition for 4 days. Immunofluorescent staining was performed with an anti-MBP, anti-Tuj1 or anti-GFAP antibody. Scale bar, 50 μm. I: The quantified graphs were determined using confocal microscopy. *P* values were obtained by Student's *t*-test (WT vs. KO). The data are shown as the mean ± standard error from three independent experiments. ***$P < 0.005$, **$P < 0.01$, *$P < 0.05$ or n.s., no significance.

down-regulated with a 1.50-fold maximum in differentiated NSCs derived from *CXXC5*$^{-/-}$ compared with differentiated cells from the *CXXC5*$^{+/+}$ mice (Supp. Info. Table 1). Among these down-regulated genes, nine (23%) oligodendrocyte marker genes, including *MBP, MAG*, and *PLP*, were identified (Supp. Info. Table 2). However, the expression of the neural marker genes, *Camk2β* and *Tuj1* (Lemetre and Zhang, 2013), and of the astrocyte markers, *Gfap* and *Bmpr1β* (Cahoy et al., 2008) were not significantly different in the *CXXC5*$^{-/-}$ and the *CXXC5*$^{+/+}$ NSCs (Supp. Info. Table 2).

The specific reductions of oligodendrocyte marker genes in differentiated NSCs from *CXXC5*$^{-/-}$ mice, such as *MBP, PLP1, MAG*, and *MOG*, but not *Tuj1*, the neural marker, and *GFAP* and *Bmpr1β*, astrocyte marker genes were further confirmed using quantitative real-time polymerase chain reaction (qRT-PCR) analysis (Fig. 2A). The mRNA expression of

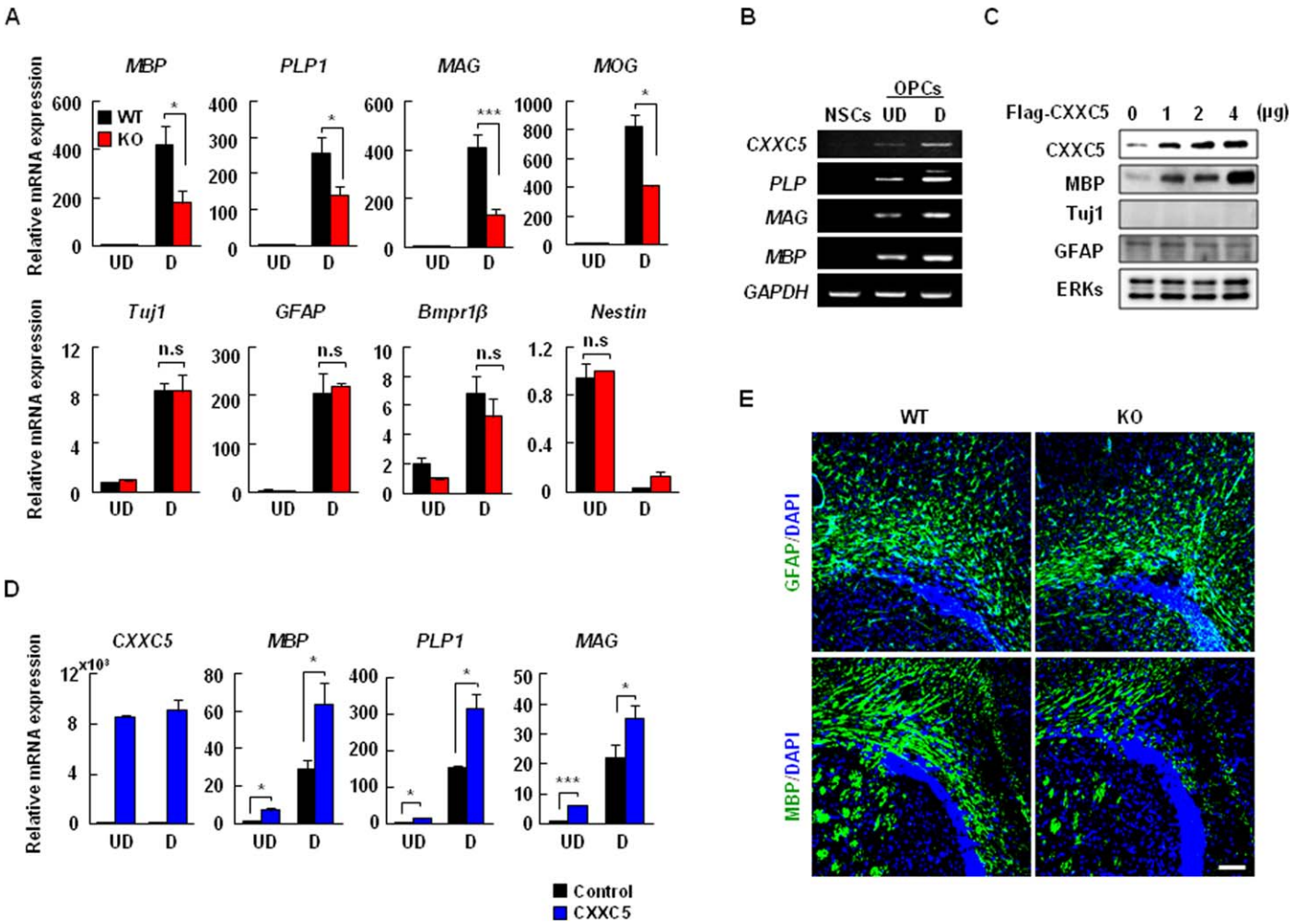

FIGURE 2: CXXC5 specifically regulates genes involved in oligodendrocyte differentiation and myelination. A: The mRNAs were isolated from NSCs grown under non-differentiation and differentiation conditions. The indicated mRNAs were detected using qRT-PCR using each primer set for the genes. Each sample was normalized to the expression of GAPDH. *P* values were obtained by Student's *t*-test (WT vs. KO). **B:** The mRNAs were isolated from the NSCs grown in non-differentiation medium and Oli-neu cells grown in non-differentiation or differentiation media. RT-PCR analyses were performed with primer sets for each gene. GAPDH was included as a loading control. **C:** NSCs were transfected with pcDNA3.1-flag-CXXC5, and cultured for 4 more days in non-differentiation medium before the cells were harvested for analyses. The indicated proteins were detected using immunoblotting. **D:** NSCs were transfected with pcDNA 3.1 or pcDNA 3.1-flag-CXXC5. The cells were further cultured in non-differentiation or differentiation media for 4 days before analyses. The indicated mRNAs were detected using qRT-PCR. *P* values were obtained by Student's *t*-test (control group vs. CXXC5 overexpression group). **E:** Coronal sections from the corpus callosum at PN14 $CXXC5^{+/+}$ mice and $CXXC5^{-/-}$ mice were stained with an anti-GFAP and anti-MBP antibody. Scale bar, 50 μm. The data represent the mean ± error of three different experiments. *P* values were obtained by Student's *t*-test. $*P<0.05$, $***P<0.005$, n.s., no significance.

nestin, a NSC marker, was decreased during differentiation; however, its level was not significantly altered during the differentiation of $CXXC5^{+/+}$ cells compared with $CXXC5^{-/-}$ cells (Fig. 2A). *CXXC5* and *MBP* mRNAs were not detected in undifferentiated NSCs. However, they were detected in the Oli-neu cell line (oligodendrocyte precursor cells [OPCs]), and levels were further increased by inducing oligodendrocyte differentiation (Fig. 2B). The role of CXXC5 in oligodendrocyte differentiation was confirmed by a dose-dependent induction of MBP by CXXC5 overexpression in NSCs grown under non-differentiation conditions (Fig. 2C). The mRNA levels of *MBP, PLP1, and MAG* were also increased by CXXC5 overexpression in NSCs, regardless of the induction of differentiation (Fig. 2D). *In vivo*, the MBP expression was significantly reduced in corpus callosum of $CXXC5^{-/-}$ mice at PN14. However, astrocytic differentiation was unaltered the loss of *CXXC5* in the corpus callosum in both the PN14 mice as determined by GFAP detection (Fig. 2E).

CXXC5 is a Transcriptional Activator of MBP

Given the nuclear localization of CXXC5 and the down-regulation of myelin gene transcription in differentiated

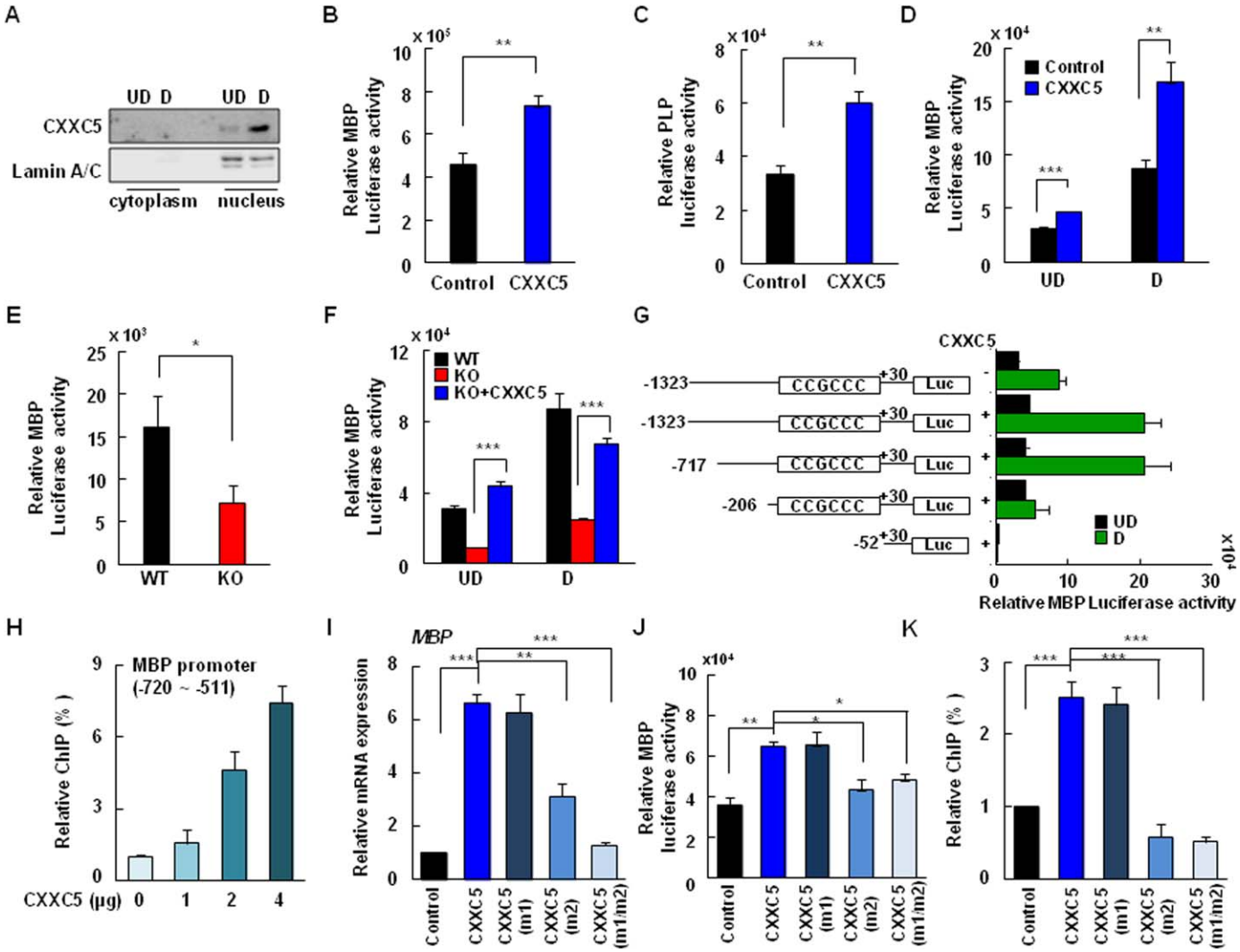

FIGURE 3: CXXC5 is a transcription factor for *MBP*. A: The whole cell extracted from NSCs was separated into nuclear and cytosolic fractions and were then subjected to immunoblot analyses to detect CXXC5 and lamin A/C. B–G: The promoter activities were analyzed by measuring luciferase activities. B, C: NSCs were transfected with pGL3-MBP (B) or pGL3-PLP1 (C) together with pcDNA 3.1-flag or pcDNA 3.1-flag-CXXC5 for 1 day, under non-differentiation conditions. *P* values were obtained by Student's *t*-test (control group *vs.* CXXC5 overexpression group). D: NSCs were transfected with pGL3-MBP together with pcDNA 3.1-flag or pcDNA 3.1-flag-CXXC5. The cells were further cultured under non-differentiation or differentiation conditions for 4 days before analyses. *P* values were obtained by Student's *t*-test (control group *vs.* CXXC5 overexpression group). E: The *CXXC5*$^{+/+}$ or *CXXC5*$^{-/-}$ NSCs were transfected with pGL3-MBP and further cultured under differentiation conditions for 4 days. *P* values were obtained by Student's *t*-test (WT vs. KO). F: NSCs isolated from *CXXC5*$^{+/+}$ mice and *CXXC5*$^{-/-}$ mice were transfected with pGL3-MBP together with pcDNA 3.1-flag or pcDNA 3.1-flag-CXXC5. The cells were further cultured under non-differentiation or differentiation conditions for 4 days before analyses. *P* values were obtained by Student's *t*-test (control group vs. CXXC5 overexpression group). G: NSCs were transfected with serially deleted pGL3-MBP together with pcDNA 3.1-flag-CXXC5. The cells were further cultured under non-differentiation or differentiation conditions for 4 days. H: NSCs were transfected with different amount of pcDNA 3.1-myc-CXXC5. The ChIP assay was performed with an anti-myc antibody using a −511 ~ −720 specific primer for the *MBP* promoter from immunoprecipitated lysates of NSCs. I-K: NSCs were transfected with pcDNA 3.1-myc-CXXC5, pcDNA 3.1-myc-CXXC5 (m1), pcDNA 3.1-myc-CXXC5 (m2), or pcDNA 3.1-myc-CXXC5 (m1/m2) for 1 day under non-differentiation conditions. I: qRT-PCR was performed for *MBP* and *CXXC5*. GAPDH was used as a loading control. J: NSCs were transfected with pGL3-MBP. Luciferase activity was performed. K: The ChIP assay was performed using −511 ~ −720-specific primers for the MBP promoter from immunoprecipitated lysates of NSCs overexpressing pcDNA 3.1-myc-CXXC5, pcDNA 3.1-myc-CXXC5 (m1), pcDNA 3.1-myc-CXXC5 (m2), or pcDNA 3.1-myc-CXXC5 (m1/m2) and further cultured for 1 day under non-differentiation conditions with an anti-myc antibody. The binding was observed by qRT-PCR. *P* values were obtained by ANOVA followed by Tukey HSD *post hoc* test [control group vs. CXXC5 overexpression group, CXXC5 vs. CXXC5(m2) or CXXC5 vs. CXXC5(m1/m2)]. The data are expressed as the mean ± standard error of three different experiments. *$P < 0.05$, and ***$P < 0.005$.

CXXC5$^{-/-}$ NSCs, we assessed the role(s) of CXXC5 as a transcriptional activator for myelin genes. The nuclear accumulation of CXXC5 in differentiated NSCs was confirmed by cell fractionation assays (Fig. 3A). The promoter activities of *MBP* and *PLP1*, as determined by individual reporters, were increased by CXXC5 overexpression in NSCs (Fig.

3B,C). Among the myelin related proteins, MBP is the most abundant in the myelin sheath (Husted, 2006; Nawaz et al., 2013). Therefore, we investigated the function of CXXC5 as a transcription factor on MBP transcription. The *MBP* promoter activity, which was increased by inducing differentiation, was further enhanced by CXXC5 overexpression in NSCs and it was reduced in differentiated in *CXXC5*$^{-/-}$ NSCs (Fig. 3D,E). In addition, the role of CXXC5 as an activator of *MBP* transcription was confirmed by rescue of the *CXXC5* knockout effect on MBP promoter activity by CXXC5 overexpression (Fig. 3F). To identify CXXC5 binding site(s) on the *MBP* promoter, we used serially deleted *MBP* promoters and measured the effects of CXXC5 overexpression. *MBP* promoter activity did not significantly change after deletion of the promoter up to position −717, regardless of the differentiation condition of the NSCs (Fig. 3G). However, promoter activity was significantly reduced, especially in differentiation-induced NSCs, when the sequence was deleted up to position −206, and activity was almost completely abolished when the promoter sequence was deleted up to position −52 (Fig. 3G).

To test for direct binding of CXXC5 to the *MBP* promoter, we divided the −720 to −191 region of the promoter, which contains the potential CXXC5 binding site, into three overlapping fragments and subjected the fragments to chromatin immunoprecipitation (ChIP) analyses. CXXC5 interacted with the −720 ∼ −511 fragment and interacted weakly with the −550 ∼ −370 fragment; however, no interaction was observed for the −410 ∼ −191 fragment (Supp. Info. Fig. 1A). The binding of CXXC5 to the −720 ∼ −511 promoter fragment, where CXXC5 showed higher affinity, was further confirmed by the dose-dependent interaction of CXXC5 with the DNA fragment in NSCs (Fig. 3H, Supp. Info. Fig. 1B).

To identify the CXXC motif(s) of CXXC5 involving *MBP* transcription, we used several mutants in which cysteines were replaced with arginines in the potential DNA-binding motifs (Supp. Info. Fig. 2A; C263/266R; *CXXC5 (m1)*, C275/278R; *CXXC5 (m2)*, and C263/266R, 275/278R; *CXXC5 (m1/m2)*). The mRNA level and promoter activity of *MBP* were increased when *CXXC5* or *CXXC5 (m1)* were overexpressed, but not when *CXXC5 (m2)* or *CXXC5 (m1/m2)* were overexpressed in the NSCs (Fig. 3I,J, Supp. Info. Fig. 2B). Moreover, the *CXXC5* (*m2*) or *CXXC5* (*m1/m2*) mutants did not bind to the −720 ∼ −511 MBP promoter fragment (Fig. 3K, Supp. Info. Fig. 2C). In NSCs grown under both non-differentiation and differentiation conditions, the increments of *MBP* promoter activity due to CXXC5 overexpression decreased when CXXC5 (m1/m2) was transfected (Supp. Info. Fig. 2D).

Using primary OPCs and Oli-neu cell lines, we further confirmed the function of CXXC5 as a transcriptional activator of *MBP* in oligodendrocyte precursor cell system. The expression of CXXC5 was increased in differentiation-induced primary OPCs and Oli-neu cells (Supp. Info. Fig. 3A,B). Both MBP mRNA and protein levels, as well as MBP promoter activity, were increased by CXXC5 overexpression in Oli-neu cells grown under non-differentiation conditions (Supp. Info. Fig. 3C–E). In addition, the binding of CXXC5 to the MBP promoter was increased in the −720 to −191 region of the promoter in Oli-neu cells (Supp. Info. Fig. 3F). Furthermore, when Oli-neu cells were grown under both non-differentiation and differentiation conditions, the increments of *MBP* promoter activity regulation by CXXC5 overexpression was not observed increment when *CXXC5* (*m1/m2*) was overexpressed (Supp. Info. Fig. 3G).

Taken together, these data indicated that CXXC5 was a transcriptional activator for *MBP* that directly interacted with the *MBP* promoter in the −720 ∼ −511 region. Furthermore, the second CXXC DNA binding motif containing cys-275 and cys-278 residues was important for transcriptional activation of the *MBP* promoter.

CXXC5 is Involved in the MBP Expression in the Corpus Callosum at PN14 Mice

To investigate the CXXC5 function *in vivo*, we performed CXXC5 expression level in various tissues. The *CXXC5* mRNA is expressed at especially high levels in components of the CNS, such as the cerebrum, cerebellum, and spinal cord (Fig. 4A). Both the mRNA and protein of CXXC5 were highly expressed in white matter, including the corpus callosum and pyramidal tract, but not in cortex (Fig. 4B,C). The mRNA levels of *CXXC5* and myelin-related genes, such as *MBP, PLP1, MAG*, and *MOG*, all increased in the brain from postnatal (PN) 14 day up to adult. The protein levels of CXXC5 and MBP also increased in a stepwise manner up to 12 weeks of age (Fig. 4D). Expression of CXXC5 was also high in regions of the brain where MBP expression is especially high such as corpus callosum (Supp. Info. Fig. 4A).

At PN14, abnormal dyscallosal (arrow) phenotype was observed together with the reduction of expressions of CXXC5 and myelin genes in the *CXXC5*$^{-/-}$ mice (Fig. 4E,F). The expression of CXXC5 observed in nuclei of cells in the corpus callosum at PN14 of *CXXC5*$^{+/+}$. The MBP expression was greatly reduced in *CXXC5*$^{-/-}$ mice (Fig. 4G). Importantly, MBP expression significantly decreased in the corpus callosum but was not significantly altered in the cortex or striatum in the *CXXC5*$^{-/-}$ mice at PN14 (Supp. Info. Fig. 4B). The expression of other myelin genes, including *PLP1, MAG*, and *MOG*, were also significantly decreased in the

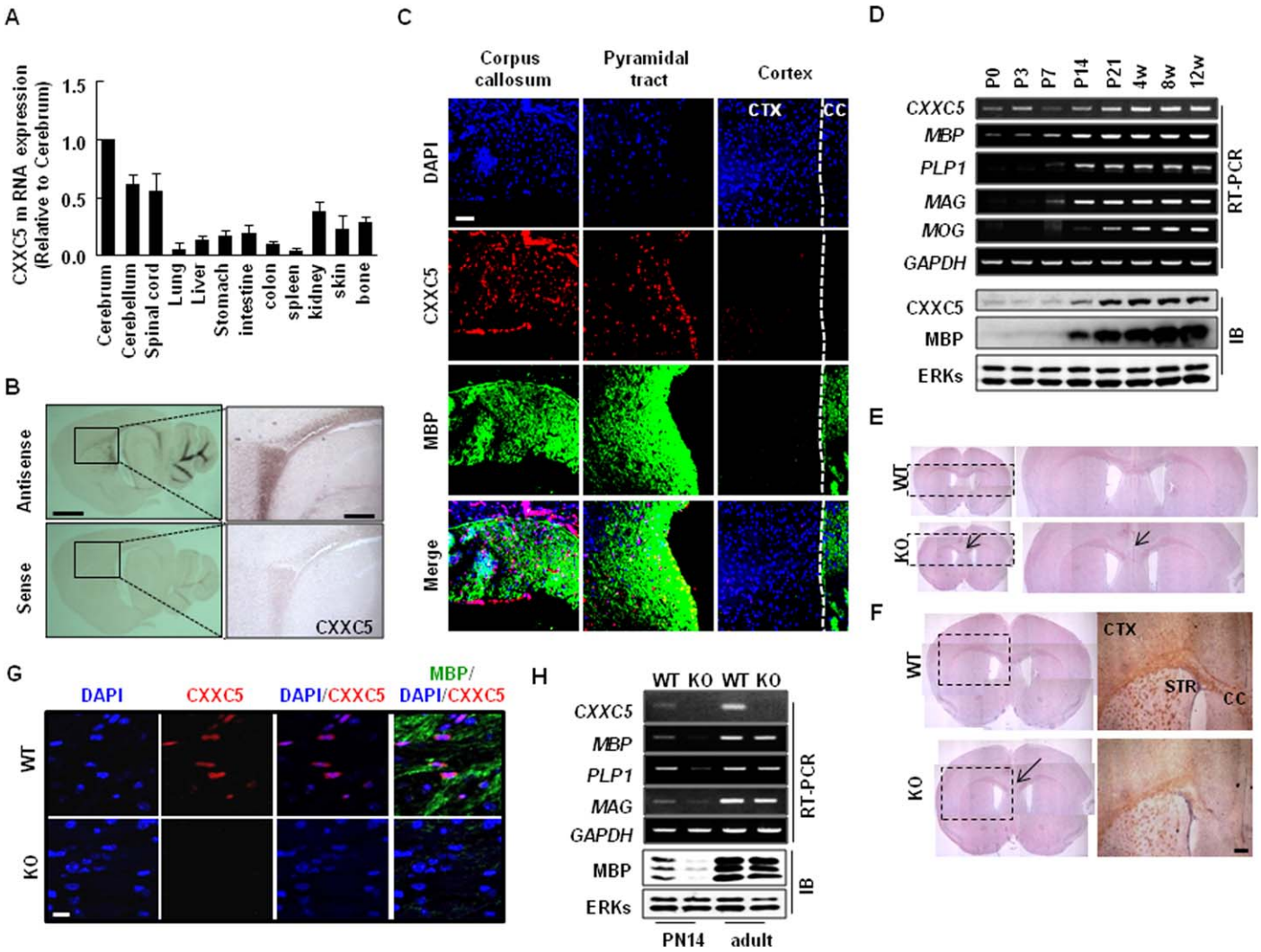

FIGURE 4: Expressions of CXXC5 and myelin genes in the white matter during the brain development, and effects of *CXXC5* knock out in myelin gene expression in the corpus callosum at PN14. A: Various tissues of 12-week-old mice were isolated, and mRNA levels of CXXC5 in each tissue were analyzed using qRT-PCR. Each sample was normalized to the expression of GAPDH. The data represent the mean ± standard error ($n = 3$). B: *In situ* hybridization was performed for CXXC5 in sagittal brain sections from 12-week-old mice. Scale bar, 2.5 mm. The boxes represent magnified images of the corpus callosum. Scale bar, 200 μm. C: Double immunofluorescent staining was performed for CXXC5 (*red*) and MBP (*green*) in the corpus callosum, pyramidal tract, and cortex from 12-week-old mouse sagittal brain sections. CTX, cortex. CC, corpus callosum. Scale bar, 50 μm. D: The mRNAs and proteins were isolated from the brains of mice at different ages. The indicated mRNAs and proteins were detected using RT-PCR and immunoblotting (IB), respectively. E, F: Coronal sections of the *CXXC5*$^{+/+}$ and *CXXC5*$^{-/-}$ mice brains at PN14 were subjected to H&E (E) and diaminobenzidine (DAB) staining with an anti-MBP antibody (F). *Arrow* indicate disrupted corpus callosum in *CXXC5*$^{-/-}$ mice brain. E: Corpus callosum is marked by dotted box and right panel showed enlarged image from dotted box. F: Left panel showed H&E stained image. Right panel showed DAB stained image from dotted box. CTX, cortex. CC, corpus callosum. STR, striatum. Scale bar, 100 μm. G: Coronal sections of *CXXC5*$^{+/+}$ mice and *CXXC5*$^{-/-}$ mice corpus callosum at PN14 were subjected to immunofluorescent staining with anti-MBP and anti-CXXC5 antibodies. scale bar, 50 μm. H: mRNAs and proteins were isolated from the corpus callosum of PN14 or adult mice, respectively. The indicated mRNAs and proteins were detected using RT-PCR and immunoblotting analyses.

corpus callosum at PN14 (Supp. Info. Fig. 4B). However, both immunohistochemical and immunoblot analyses showed that the expression level of MBP in the corpus callosum recovered to the approximate levels of the *CXXC5*$^{+/+}$ adult mice (Fig. 4H, Supp. Info. Fig. 4C). The expression of other myelin genes, including *MAG* and *PLP1*, in the corpus callosum also recovered in the adult mice (Fig. 4H).

CXXC5 is Important for Axon Myelination and Structural Integrity of Myelin Sheath Structure

MBP and other myelin proteins involved in myelination maintain the structure and stability of the myelin sheath by holding the myelin bilayers together (Min et al., 2009). To characterize the myelination defect in the *CXXC5*$^{-/-}$ mice in detail, we analyzed the myelin structure in the corpus callosum of the mice at

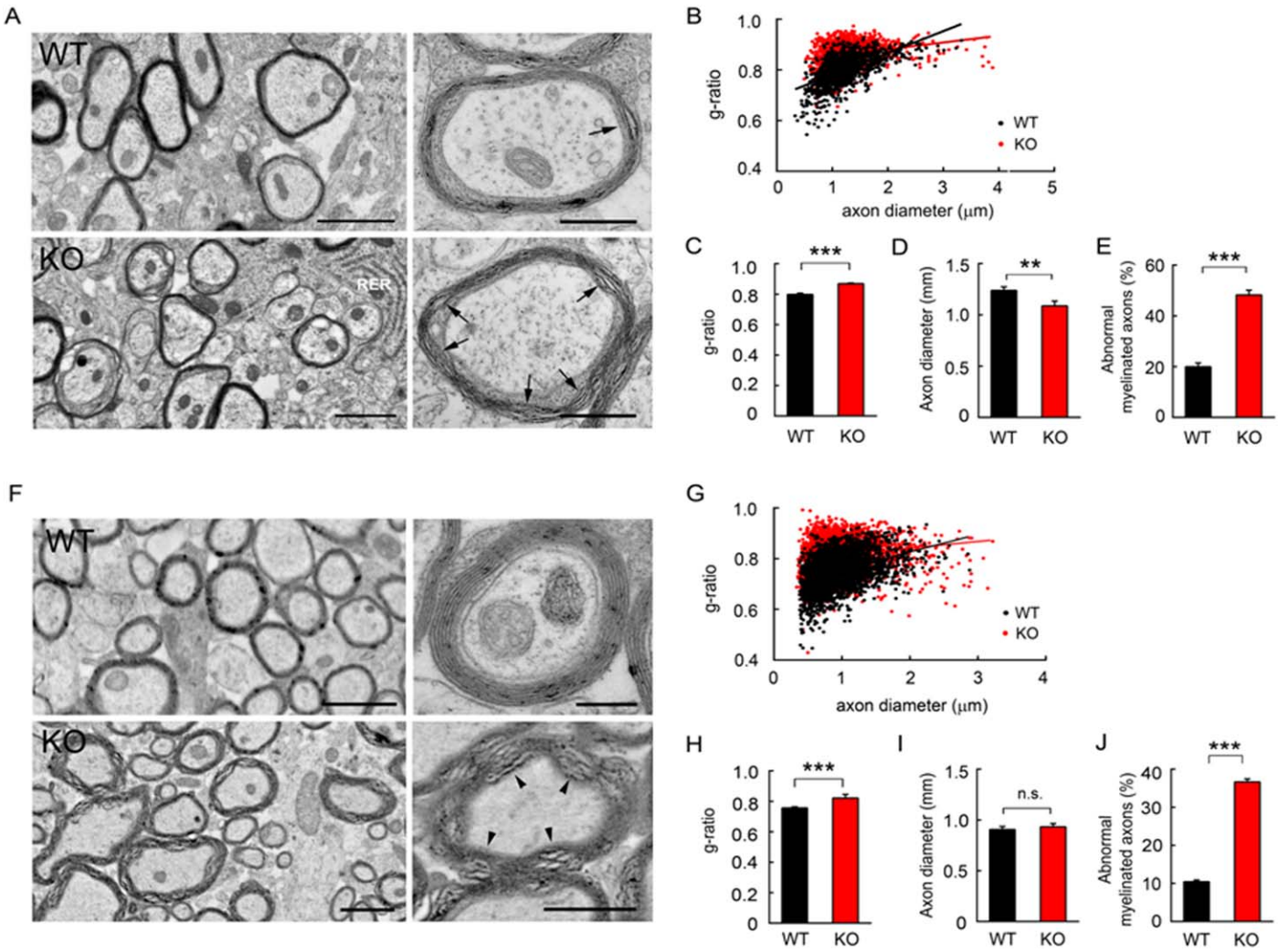

FIGURE 5: CXXC5 knockout impairs myelin structure in the corpus callosum. A–J: Electron microscopy of corpus callosum of *CXXC5*$^{+/+}$ and *CXXC5*$^{-/-}$ mice. The analysis was performed on PN14 (A-E) and 12-week-old mice (F-J). Representative electron micrographs from *CXXC5*$^{+/+}$ and *CXXC5*$^{-/-}$ mice at PN14 (A) and 12 weeks (F), respectively (scale bar, 1 μm). The right panels are higher magnification images (scale bar, 500 nm). The arrows and arrowheads point to aberrantly loosened, bulged regions of myelin sheets. B, G: Scatter plot of g-ratio values for the *CXXC5*$^{+/+}$ (*black dots*) and *CXXC5*$^{-/-}$ (*red dots*) corpus callosum. C, H: The bar graphs show the average g-ratio. D, I: The average diameter of myelinated axons. E, J: The percentage of abnormally myelinated axons. For each genotype, we measured >1000 axons and >3000 axons in three mice each of PN14 and 12-week-old animals, respectively. *P* values were obtained by Student's *t*-test (WT vs. KO). The data represent the mean ± standard error. **P* < 0.05, ***P* < 0.01, ****P* < 0.005, n.s., no significance.

PN14 and 12 weeks of age via electron microscopy. At PN14, several abnormalities were observed in the *CXX5*$^{-/-}$ mice, such as thinning of axonal myelin sheaths, undulating myelin layers, and split myelin lamellae associated with myelin outfolding (Fig. 5A). We also observed that the g-ratio, which is the ratio of the inner axonal diameter to the total outer diameter, was increased in the PN14 *CXXC5*$^{-/-}$ mice compared with the *CXXC5*$^{+/+}$ mice (Fig. 5B,C). The average *g*-ratio of 0.80 ± 0.006 ($n = 1110$) of the wild-type mice increased to 0.87 ± 0.003 ($n = 1211$) in the *CXXC*$^{-/-}$ mice (Fig. 5C; $P = 0.00035$). Moreover, a slight reduction of axonal diameter was observed in the *CXXC*$^{-/-}$ mice (1.09 ± 0.047 μm, $n = 1211$) compared with the *CXXC5*$^{+/+}$ mice (1.24 ± 0.034 μm, $n = 1110$), (Fig. 5D, $P = 0.0053$). Furthermore, the *CXXC*$^{-/-}$ mice had a significantly higher percentage of aberrantly myelinated axons ($48.3\% \pm 1.9\%$, $n = 90$ micrographs) than did the *CXXC*$^{+/+}$ mice ($20.0\% \pm 1.5\%$, $n = 90$ micrographs) (Fig. 5E).

At 12 weeks of age, when MBP expression levels recovered to the levels of the wild-type mice (Fig. 4H), abnormalities in myelin the sheet structure and thickness, as observed at PN14, persisted in the *CXX5*$^{-/-}$ mice (Fig. 5F). Furthermore, the g-ratio remained abnormally high regardless of axonal diameter in the *CXXC5*$^{-/-}$ mice compared with the *CXXC5*$^{+/+}$ mice (Fig. 5G,H). The *g*-ratios were 0.76 ± 0.007 ($n = 3171$) and 0.82 ± 0.011 ($n = 3070$) for the *CXXC5*$^{+/+}$ mice and the *CXXC5*$^{-/-}$ mice, respectively (Fig. 5H, $P = 0.0002$). There

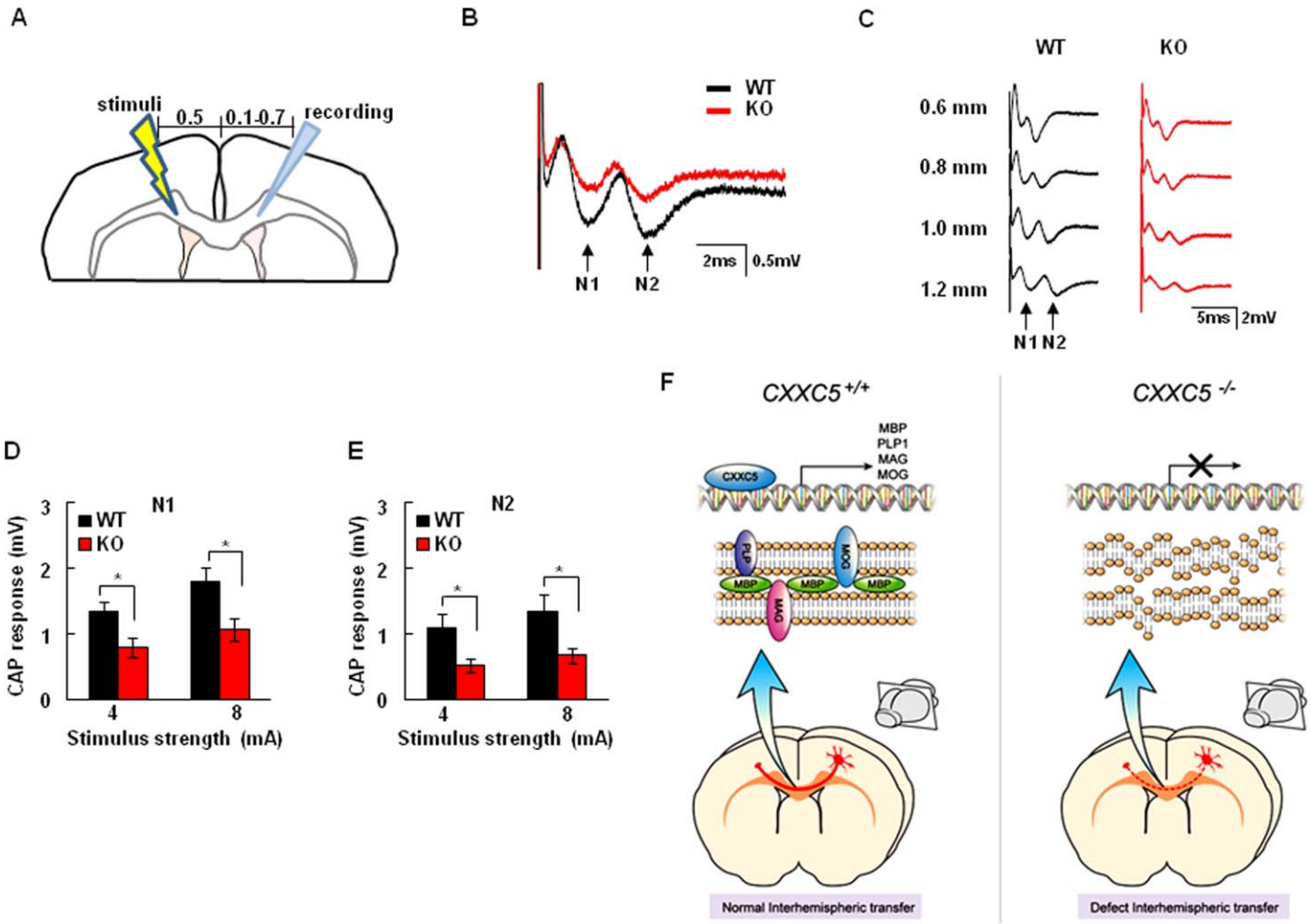

FIGURE 6: CXXC5 knockout decreases conduction amplitude in the corpus callosum. A: Positions of two electrodes in coronal brain slices of 12-week-old mouse are illustrated. **B:** Representative traces of CAP amplitudes of *CXXC5*$^{+/+}$ and *CXXC5*$^{-/-}$ mice in corpus callous for 1.0 mm distance between two electrodes. **C:** Representative trace of evoked CAPs in corpus callosum for different distances between two electrodes (0.6, 0.8, 1.0, or 1.2 mm) in *CXXC5*$^{+/+}$ ($n = 14$; from 5 animals) and *CXXC5*$^{-/-}$ ($n = 12$; from 4 animals) brain slices. The *arrows* represent peaks of N1 and N2. **D, E:** The bar graphs show the CAP response amplitudes of N1 (D) and N2 (E) in *CXXC5*$^{+/+}$ ($n = 13$; from 6 animals) and *CXXC5*$^{-/-}$ ($n = 12$; from 7 animals) mice. **F:** Schematic representation of a proposed model for the role of CXXC5 in myelination. In *CXXC5*$^{+/+}$ mice, transcriptionally induced myelin proteins (MBP, PLP, MAG, and MOG) in early brain developmental play roles in the integration of normal myelin structure in the corpus callosum. In *CXXC5*$^{-/-}$ mice, reduced expressions of the myelin proteins by CXXC5 loss leads to the formation of abnormal myelin structure such as undulating myelin layers and outfolding of myelin lamellae. The persistent of the abnormal myelin structure in adulthood hampers interhemispheric information transfer at corpus callosum. The data represent the mean ± standard error. *P* values were obtained by Student's *t*-test. **P* < 0.05, n.s., no significance.

were no significant differences in axonal diameter between the *CXXC5*$^{+/+}$ mice (0.91 ± 0.037 μm, $n = 3171$) and the *CXXC5*$^{-/-}$ mice (0.93 ± 0.033 μm, $n = 3071$), (Fig. 5I, $P = 0.252$). However, the *CXXC*$^{-/-}$ mice (36.7% ± 0.8%, $n = 170$ micrographs) had a higher percentage of aberrantly myelinated axons than did the *CXXC*$^{+/+}$ mice (10.5% ± 0.4%, $n = 170$ micrographs) (Fig. 5J).

Electric Conduction in the Corpus Callosum is Reduced in CXXC5$^{-/-}$ *Mice*

The integrity of the myelin sheath in normal myelination is essential for normal information transfer in the brain, and demyelination in the corpus callosum can result in a delay and decrease in amplitude of the compound action potential (CAP) (Crawford et al., 2009a; Ruff et al., 2013). We therefore addressed the question of whether anatomically abnormal myelination in *CXXC5*$^{-/-}$ mice (Fig. 5) can lead to impaired callosal conduction. To this end, CAP, which is widely used for characterizing conduction properties of axons (Golden et al., 2011), was measured from mouse brain slices. The CAP response in acutely dissociated brain slices was recorded using an electrophysiological measurement by placing two electrodes in the corpus callosum, as illustrated in Fig. 6A. We observed an evoked CAP response in the corpus callosum

consisting of two negative peak components reflecting two different populations of axons; fast (N1) and slow (N2) conducting axons (Fig. 6B). At each position, the amplitudes of two negative peak components in *CXXC5*$^{+/+}$ and *CXXC5*$^{-/-}$ mice were significantly changed (Fig. 6B,C). The CAP response amplitudes of N1 and N2 were significantly reduced for a given stimuli in the *CXXC5*$^{-/-}$ mice compared with that of the *CXXC5*$^{+/+}$ mice [(N1–4 mA; 0.796 ± 0.1448 mV vs. 1.333 ± 0.1455 mV, 8 mA; 1.085 ± 0.1620 mV vs. 1.564 ± 0.2192 mV) and (N2–4 mA; 0.524 ± 0.1113 mV vs. 1.092 ± 0.2188 mV, 8 mA; 0.672 ± 0.1228 mV vs. 1.340 ± 0.2754 mV)] (Fig. 6D,E). However, there were no significant differences in the latencies to reach the negative peaks (N1 and N2) or in the conduction velocities (Supp. Info. Fig.5A,B) and in the refractoriness of callosal conduction between the CXXC5$^{+/+}$ and CXXC5$^{-/-}$ mice (N1; 0.625 ± 0.0398 m/s vs. 0.699 ± 0.0577 m/s and N2; 0.279 ± 0.0087 m/s vs. 0.280 ± 0.0116 m/s) (Supp. Info. Fig.5C-E). Overall, abnormal myelination in the corpus callosum in the *CXXC5*$^{-/-}$ mice decreases the amplitude of the CAP response.

Discussion

Because the myelin sheath is essential for proper functioning of the nervous system, oligodendrocyte differentiation and myelination are important processes during brain development. Myelination during early brain development is responsible for the structural integrity of the myelin sheath. Multiple genes, including *MBP*, *PLP*, *MAG*, and *MOG*, are important for structural integrity, including the compactness of myelin, which involves the binding of proteins with the lipids of the myelin membrane. Abnormalities in the gene expression or composition of differentiating oligodendrocytes can result in neurologic diseases, such as multiple sclerosis (Caprariello et al., 2012; Prineas and Parratt, 2012), leukodystrophy (Webber et al., 2009), and psychiatric disorders (Edgar et al., 2011; Gutierrez-Fernandez et al., 2010; Hayashi et al., 2011; Shimizu et al., 2014). Therefore, the identification and characterization of the genes for regulatory factors involved in myelination are important for understanding the mechanisms of neurological disorders, as well as for the development of therapeutic strategies for these disorders.

Wnt/β-catenin signaling is important for brain development. Ligands and signaling components of Wnt/β-catenin pathway such as Wnt1, Wnt3, Wnt3a, Fzd1, Fzd2, or Fzd3 are expressed in the telencephalon development (Fischer et al., 2007; Parr et al., 1993), and those are involved in the forebrain patterning or fate decision of radial glia and intermediated progenitor cells (Harrison-Uy and Pleasure, 2012; Takebayashi and Ikenaka, 2015). In addition, a role of the Wnt/β-catenin signaling in the myelination was identified that the number of PLP-positive differentiated oligodendrocytes was significantly decreased in Olig1-Cre/β-catenin signaling KO spinal cord (Dai et al., 2014). Expressions of the myelin genes such as PLP and MBP were increased by lithium chloride-induced activation of Wnt/β-catenin signaling in oligodendroyctes (Meffre et al., 2015). However, a mechanism for the transcriptional activation of myelin genes was not illustrated.

In the present study, we demonstrated that CXXC5 is an important transcription factor that controlled MBP expression during oligodendrocyte differentiation. In addition, using both *in vitro* and *in vivo* analyses, we further demonstrated that CXXC5 was an important myelination factor, controlling multiple genes involved in myelination. The most prominent abnormal feature with respect to myelin-related proteins in the *CXXC5*$^{-/-}$ mice was the abnormal myelin structure. Supporting the importance of activating myelin gene expression in the structural integrity of myelin, structural defects of the myelin sheath were found in the *MBP* deficient *shiverer* mice (Popko et al., 1987) and *PLP* knockout mice (Baumann and Pham-Dinh, 2001) such as *CXXC5*$^{-/-}$ mice. The timing of myelin gene expression is also important in the integrity of myelin (Kuronen et al., 2012). The recovery of myelin gene expression without restoration of myelin structure also occurred in the adult brain of *Cln8*-deficient mice, which also revealed a loss of myelin gene expression in early development (Kuronen et al., 2012). The loss of *MBP* expression and other myelin genes, including *MAG*, *PLP*, and *MOG*, in the early developmental stages of the *CXXC5*$^{-/-}$ mice were recovered in adulthood. However, the structural defects of myelin were not restored. Therefore, the regulation of myelin gene expression by CXXC5 in early brain development is important for forming normal myelin structure. But, a mechanism for the recovery of myelin gene expression in adult *CXXC5*$^{-/-}$ mice is unclear but may involve an adaptive mechanism occurring independently of CXXC5.

Corpus callosum is important for transferring the electrical signal of neuron through myelinated axons (Tomasch, 1954). The defect or abnormal myelin structure of corpus callosum is associated with reduction of electrical properties and it causes mental or physical impairment in neurological disorders such as schizophrenia, autism or bipolar disorder (Bakiri et al., 2011; Paul et al., 2007). Although the functional interhemispheric connectivity was found to be important for controlling callosal signal transfer and complex brain function (van der Knaap and van der Ham, 2011), the regulation factors of myelination on the corpus callosum is poorly understood. We found that the decreased conduction amplitude in the *CXXC5*$^{-/-}$ corpus callosum, which exhibited aberrant myelin structure, indicated that the structural integrity of myelin in the corpus callosum is important for normal interhemispheric information transfer.

The conduction velocity of CAP is reflected by the diameter of nerve fibers (De Luca et al., 1987; Morita et al., 2002) and the amplitude of CAP is dependent on the duration of stimuli of single nerve fiber action potential and

myelination (Olney et al., 1987). In *CXXC5*$^{-/-}$ adult mice, did not show any change on axon diameter and expression of myelin genes, but still showed disruption of myelin structure, differently with P14 mice. These data provides reasons that the conduction velocity was not changed even though the electrical amplitude was changed in *CXXC5*$^{-/-}$ mice. Similar to our *CXXC5*$^{-/-}$ mice phenotypes, several previous studies also showed the changes in electrical amplitude with major deficits in myelination (Crawford et al., 2009a,b).

Overall, control of the expression of myelin genes by CXXC5 in early brain development was important for structural integrity which is involving the transfer of electrical signals in the corpus callosum (Fig. 6F). Together, we identified a key regulatory factor controlling multiple myelin genes. In addition, as far as we know, this is the first study to report a role of CXXC5 on myelination at corpus callosum.

Acknowledgment

Grant sponsor: National Research Foundation of Korea (NRF) of Korea government (MEST); Grant numbers: 2009-0083522; 2010-0020235; 2015R1A2A1A05001873; Grant sponsor: Brain Korea (BK) 21 Plus studentship.

Author Contributions

K.-Y.C supervised the study, interpreted data, and wrote the manuscript. M.-Y.K designed the experiments, performed most of the experiments and wrote the manuscript. H.-Y.K helped to design and interpreted results. J.H and D.K performed and analyzed mice behavior test. H.L and E.C performed and analyzed electrophysiological experiments. Y.L and J.R performed electron microscopic analysis. D.G.K helped and provided idea about mice behavior test. D.S.M provided reagents, comments and discussion.

References

Aggarwal S, Yurlova L, Simons M. 2011. Central nervous system myelin: Structure, synthesis and assembly. Trends Cell Biol 21:585–593.

Andersson T, Sodersten E, Duckworth JK, Cascante A, Fritz N, Sacchetti P, Cervenka I, Bryja V, Hermanson O. 2009. CXXC5 is a novel BMP4-regulated modulator of Wnt signaling in neural stem cells. J Biol Chem 284:3672–3681.

Aras S, Pak O, Sommer N, Finley R, Jr., Huttemann M, Weissmann N, Grossman LI. 2013. Oxygen-dependent expression of cytochrome c oxidase subunit 4-2 gene expression is mediated by transcription factors RBPJ, CXXC5 and CHCHD2. Nucleic Acids Res 41:2255–2266.

Bakiri Y, Karadottir R, Cossell L, Attwell D. 2011. Morphological and electrical properties of oligodendrocytes in the white matter of the corpus callosum and cerebellum. J Physiol 589:559–573.

Baumann N, Pham-Dinh D. 2001. Biology of oligodendrocyte and myelin in the mammalian central nervous system. Physiol Rev 81:871–927.

Bottomly D, Kyler SL, McWeeney SK, Yochum GS. 2010. Identification of {beta}-catenin binding regions in colon cancer cells using ChIP-Seq. Nucleic Acids Res 38:5735–5745.

Brambilla P, Bellani M, Yeh PH, Soares JC. 2009. Myelination in bipolar patients and the effects of mood stabilizers on brain anatomy. Curr Pharm Des 15:2632–2636.

Cahoy JD, Emery B, Kaushal A, Foo LC, Zamanian JL, Christopherson KS, Xing Y, Lubischer JL, Krieg PA, Krupenko SA, Thompson WJ, Barres BA. 2008. A transcriptome database for astrocytes, neurons, and oligodendrocytes: A new resource for understanding brain development and function. J Neurosci 28:264–278.

Caprariello AV, Mangla S, Miller RH, Selkirk SM. 2012. Apoptosis of oligodendrocytes in the central nervous system results in rapid focal demyelination. Ann Neurol 72:395–405.

Chew LJ, Coley W, Cheng Y, Gallo V. 2010. Mechanisms of regulation of oligodendrocyte development by p38 mitogen-activated protein kinase. J Neurosci 30:11011–11027.

Cokol M, Nair R, Rost B. 2000. Finding nuclear localization signals. EMBO Rep 1:411–415.

Crawford DK, Mangiardi M, Tiwari-Woodruff SK. 2009a. Assaying the functional effects of demyelination and remyelination: Revisiting field potential recordings. J Neurosci Methods 182:25–33.

Crawford DK, Mangiardi M, Xia X, Lopez-Valdes HE, Tiwari-Woodruff SK. 2009b. Functional recovery of callosal axons following demyelination: A critical window. Neuroscience 164:1407–1421.

Dai ZM, Sun S, Wang C, Huang H, Hu X, Zhang Z, Lu QR, Qiu M. 2014. Stage-specific regulation of oligodendrocyte development by Wnt/beta-catenin signaling. J Neurosci 34:8467–8473.

De Luca CJ, Bloom LJ, Gilmore LD. 1987. Compression induced damage on in-situ severed and intact nerves. Orthopedics 10:777–784.

Deber CM, Reynolds SJ. 1991. Central nervous system myelin: Structure, function, and pathology. Clin Biochem 24:113–134.

Edgar NM, Touma C, Palme R, Sibille E. 2011. Resilient emotionality and molecular compensation in mice lacking the oligodendrocyte-specific gene Cnp1. Transl Psychiatry 1:e42.

Fischer T, Guimera J, Wurst W, Prakash N. 2007. Distinct but redundant expression of the Frizzled Wnt receptor genes at signaling centers of the developing mouse brain. Neuroscience 147:693–711.

Golden SA, Covington HE, 3rd, Berton O Russo SJ. 2011. A standardized protocol for repeated social defeat stress in mice. Nat Protoc 6:1183–1191.

Guo F, Lang J, Sohn J, Hammond E, Chang M, Pleasure D. 2015. Canonical Wnt signaling in the oligodendroglial lineage-puzzles remain. Glia 63:1671–1693.

Gutierrez-Fernandez A, Gonzalez-Pinto A, Vega P, Barbeito S, Matute C. 2010. Expression of oligodendrocyte and myelin genes is not altered in peripheral blood cells of patients with first-episode schizophrenia and bipolar disorder. Bipolar Disord 12:107–109.

Haroutunian V, Katsel P, Roussos P, Davis KL, Altshuler LL, Bartzokis G. 2014. Myelination, oligodendrocytes, and serious mental illness. Glia 62:1856–1877.

Harrison-Uy SJ, Pleasure SJ. 2012. Wnt signaling and forebrain development. Cold Spring Harb Perspect Biol 4:a008094.

Hayashi Y, Nihonmatsu-Kikuchi N, Yu X, Ishimoto K, Hisanaga SI, Tatebayashi Y. 2011. A novel, rapid, quantitative cell-counting method reveals oligodendroglial reduction in the frontopolar cortex in major depressive disorder. Mol Psychiatry 16:1155–1158.

Husted C. 2006. Structural insight into the role of myelin basic protein in multiple sclerosis. Proc Natl Acad Sci USA 103:4339–4340.

Inouye H, Kirschner DA. 1991. Folding and function of the myelin proteins from primary sequence data. J Neurosci Res 28:1–17.

Jeon BN, Yoo JY, Choi WI, Lee CE, Yoon HG, Hur MW. 2008. Proto-oncogene FBI-1 (Pokemon/ZBTB7A) represses transcription of the tumor suppressor Rb gene via binding competition with Sp1 and recruitment of co-repressors. J Biol Chem 283:33199–33210.

Jeong WJ, Yoon J, Park JC, Lee SH, Kaduwal S, Kim H, Yoon JB, Choi KY. 2012. Ras stabilization through aberrant activation of Wnt/beta-catenin signaling promotes intestinal tumorigenesis. Sci Signal 5:ra30.

Jung M, Kramer E, Grzenkowski M, Tang K, Blakemore W, Aguzzi A, Khazaie K, Chlichlia K, von Blankenfeld G, Kettenmann H. 1995. Lines of murine oligodendroglial precursor cells immortalized by an activated neu tyrosine kinase show distinct degrees of interaction with axons in vitro and in vivo. Eur J Neurosci 7:1245–1265.

Kim MS, Yoon SK, Bollig F, Kitagaki J, Hur W, Whye NJ, Wu YP, Rivera MN, Park JY, Kim HS, Malik K, Bell DW, Englert C, Perantoni AO, Lee SB. 2010a. A novel Wilms tumor 1 (WT1) target gene negatively regulates the WNT signaling pathway. J Biol Chem 285:14585–14593.

Kim MY, Kaduwal S, Yang DH, Choi KY. 2010b. Bone morphogenetic protein 4 stimulates attachment of neurospheres and astrogenesis of neural stem cells in neurospheres via phosphatidylinositol 3 kinase-mediated upregulation of N-cadherin. Neuroscience 170:8–15.

Kim MY, Moon BS, Choi KY. 2013. Isolation and maintenance of cortical neural progenitor cells in vitro. Methods Mol Biol 1018:3–10.

Kim HY, Yang DH, Shin SW, Kim MY, Yoon JH, Kim S, Park HC, Kang DW, Min D, Hur MW, Choi KY. 2014. CXXC5 is a transcriptional activator of Flk-1 and mediates bone morphogenic protein-induced endothelial cell differentiation and vessel formation. Faseb J 28:615–626.

Kim HY, Yoon JY, Yun JH, Cho KW, Lee SH, Rhee YM, Jung HS, Lim HJ, Lee H, Choi J, Heo JN, Lee W, No KT, Min D, Choi KY. 2015. CXXC5 is a negative-feedback regulator of the Wnt/beta-catenin pathway involved in osteoblast differentiation. Cell Death Differ 22:912–920.

Kuronen M, Hermansson M, Manninen O, Zech I, Talvitie M, Laitinen T, Grohn O, Somerharju P, Eckhardt M, Cooper JD, Lehesjoki AE, Lahtinen U, Kopra O. 2012. Galactolipid deficiency in the early pathogenesis of neuronal ceroid lipofuscinosis model Cln8mnd: Implications to delayed myelination and oligodendrocyte maturation. Neuropathol Appl Neurobiol 38:471–486.

Langseth AJ, Munji RN, Choe Y, Huynh T, Pozniak CD, Pleasure SJ. 2010. Wnts influence the timing and efficiency of oligodendrocyte precursor cell generation in the telencephalon. J Neurosci 30:13367–13372.

Lee JC, Mayer-Proschel M, Rao MS. 2000. Gliogenesis in the central nervous system. Glia 30:105–121.

Lemetre C, Zhang ZD. 2013. A brief introduction to tiling microarrays: Principles, concepts, and applications. Methods Mol Biol 1067:3–19.

Mahon K, Burdick KE, Szeszko PR. 2010. A role for white matter abnormalities in the pathophysiology of bipolar disorder. Neurosci Biobehav Rev 34:533–554.

Makoukji J, Shackleford G, Meffre D, Grenier J, Liere P, Lobaccaro JM, Schumacher M, Massaad C. 2011. Interplay between LXR and Wnt/beta-catenin signaling in the negative regulation of peripheral myelin genes by oxysterols. J Neurosci 31:9620–9629.

Matigian N, Windus L, Smith H, Filippich C, Pantelis C, McGrath J, Mowry B, Hayward N. 2007. Expression profiling in monozygotic twins discordant for bipolar disorder reveals dysregulation of the WNT signalling pathway. Mol Psychiatry 12:815–825.

Meffre D, Massaad C, Grenier J. 2015. Lithium chloride stimulates PLP and MBP expression in oligodendrocytes via Wnt/beta-catenin and Akt/CREB pathways. Neuroscience 284:962–971.

Min Y, Kristiansen K, Boggs JM, Husted C, Zasadzinski JA, Israelachvili J. 2009. Interaction forces and adhesion of supported myelin lipid bilayers modulated by myelin basic protein. Proc Natl Acad Sci USA 106:3154–3159.

Morita G, Tu YX, Okajima Y, Honda S, Tomita Y. 2002. Estimation of the conduction velocity distribution of human sensory nerve fibers. J Electromyogr Kinesiol 12:37–43.

Nawaz S, Schweitzer J, Jahn O, Werner HB. 2013. Molecular evolution of myelin basic protein, an abundant structural myelin component. Glia 61: 1364–1377.

Olney RK, Budingen HJ, Miller RG. 1987. The effect of temporal dispersion on compound action potential area in human peripheral nerve. Muscle Nerve 10:728–733.

Parr BA, Shea MJ, Vassileva G, McMahon AP. 1993. Mouse Wnt genes exhibit discrete domains of expression in the early embryonic CNS and limb buds. Development 119:247–261.

Paul LK, Brown WS, Adolphs R, Tyszka JM, Richards LJ, Mukherjee P, Sherr EH. 2007. Agenesis of the corpus callosum: Genetic, developmental and functional aspects of connectivity. Nat Rev Neurosci 8:287–299.

Paus T, Toro R. 2009. Could Sex Differences in White Matter be Explained by g ratio? Front Neuroanat 3:14.

Pendino F, Nguyen E, Jonassen I, Dysvik B, Azouz A, Lanotte M, Segal-Bendirdjian E, Lillehaug JR. 2009. Functional involvement of RINF, retinoid-inducible nuclear factor (CXXC5), in normal and tumoral human myelopoiesis. Blood 113:3172–3181.

Popko B, Puckett C, Lai E, Shine HD, Readhead C, Takahashi N, Hunt SW, 3rd, Sidman RL Hood L. 1987. Myelin deficient mice: Expression of myelin basic protein and generation of mice with varying levels of myelin. Cell 48: 713–721.

Prineas JW, Parratt JD. 2012. Oligodendrocytes and the early multiple sclerosis lesion. Ann Neurol 72:18–31.

Richardson WD, Kessaris N, Pringle N. 2006. Oligodendrocyte wars. Nat Rev Neurosci 7:11–18.

Rosenbluth J, Nave KA, Mierzwa A, Schiff R. 2006. Subtle myelin defects in PLP-null mice. Glia 54:172–182.

Ruff CA, Ye H, Legasto JM, Stribbell NA, Wang J, Zhang L, Fehlings MG. 2013. Effects of adult neural precursor-derived myelination on axonal function in the perinatal congenitally dysmyelinated brain: Optimizing time of intervention, developing accurate prediction models, and enhancing performance. J Neurosci 33:11899–11915.

Seiwa C, Sugiyama I, Yagi T, Iguchi T, Asou H. 2000. Fyn tyrosine kinase participates in the compact myelin sheath formation in the central nervous system. Neurosci Res 37:21–31.

Shimizu S, Koyama Y, Hattori T, Tachibana T, Yoshimi T, Emoto H, Matsumoto Y, Miyata S, Katayama T, Ito A, Tohyama M. 2014. DBZ, a CNS-specific DISC1 binding protein, positively regulates oligodendrocyte differentiation. Glia 62:709–724.

Takebayashi H, Ikenaka K. 2015. Oligodendrocyte generation during mouse development. Glia 63:1350–1356.

Tawk M, Makoukji J, Belle M, Fonte C, Trousson A, Hawkins T, Li H, Ghandour S, Schumacher M, Massaad C. 2011. Wnt/beta-catenin signaling is an essential and direct driver of myelin gene expression and myelinogenesis. J Neurosci 31:3729–3742.

Tomasch J. 1954. Size, distribution, and number of fibres in the human corpus callosum. Anat Rec 119:119–135.

van der Knaap LJ, van der Ham IJ. 2011. How does the corpus callosum mediate interhemispheric transfer? A review. Behav Brain Res 223: 211–221.

Vourc'h P, Martin I, Marouillat S, Adrien JL, Barthelemy C, Moraine C, Muh JP, Andres C. 2003. Molecular analysis of the oligodendrocyte myelin glycoprotein gene in autistic disorder. Neurosci Lett 338:115–118.

Webber DJ, van Blitterswijk M, Chandran S. 2009. Neuroprotective effect of oligodendrocyte precursor cell transplantation in a long-term model of periventricular leukomalacia. Am J Pathol 175:2332–2342.

Wei Q, Miskimins WK, Miskimins R. 2003. The Sp1 family of transcription factors is involved in p27(Kip1)-mediated activation of myelin basic protein gene expression. Mol Cell Biol 23:4035–4045.

Yang DH, Yoon JY, Lee SH, Bryja V, Andersson ER, Arenas E, Kwon YG, Choi KY. 2009. Wnt5a is required for endothelial differentiation of embryonic stem cells and vascularization via pathways involving both Wnt/beta-catenin and protein kinase Calpha. Circ Res 104:372–379.

Zhang M, Wang R, Wang Y, Diao F, Lu F, Gao D, Chen D, Zhai Z, Shu H. 2009. The CXXC finger 5 protein is required for DNA damage-induced p53 activation. Sci China C Life Sci 52:528–538.